Small-Signal Stability Analysis and Circulating Currents Suppression of Grid-Forming Converter Cluster Delivery Systems

Hangyu Chen, Kehao Zhuang, Liangxiao Luo, Verena Häberle, Huanhai Xin, Linbin Huang

***Abstract*—In future converter-based power systems, grid-forming converters (GFMCs) have been regarded as promising devices for enhancing the system strength. Due to the limited capacity of electronic devices, a large number of GFMC modules are usually aggregated to achieve better performance. However, GFMC aggregations often experience significant circulating current when connected to the grid. In this paper, we first establish the closed-loop model of a GFMC cluster delivery system (CDS), which aggregates multiple GFMC modules. Using matrix eigenvalue decomposition, we decouple the CDS into two systems. We find that one of them determines the circulating currents, while the other reflects the dynamics between the CDS and the infinite bus. Based on our analysis, we propose an approach to guide the suppression of circulating currents in CDS. Simulation results validate the effectiveness of the proposed analysis and approach, showing significant improvements in circulating currents suppression in CDSs.**

***Index Terms*—Suppression, circulating currents, grid-forming converter, cluster delivery system.**

I. INTRODUCTION

With the increasing integration of converter-based devices, the power system gradually loses its original physical inertia, which poses many challenges for power system operation and control [1]. Grid-forming converters (GFMCs) are proposed to strengthen the power system because of their voltage-source-like properties [2]. GFMCs are usually aggregated and connected to the grid, which expands the capacity to achieve expected performance in the resulting GFMC cluster delivery system (CDS), e.g., a renewable generation unit [3], a transmission regulation unit [4], or a virtual power plant for dynamic ancillary services provision [5], [6]. Due to the differences in the power network topology and GFMC configuration in the CDS, the GFMC cluster's collective behavior is constrained, and circulating currents within the cluster are generally inevitable. Such circulating currents not only lead to overheating losses at the device level but also to oscillations and instability at the system level [7]–[10].

To analyze circulating currents in CDS, today's research focuses on CDS's small-signal stability by using state-space theory [7] and impedance-based theory [8]. To mitigate circulating currents in CDS, either communication-based or communication-free methods are typically considered. The former utilizes global information for controlling the CDS [9]. The latter, which are more commonly used virtual impedance [8] or adjust the power network parameters between the GFMCs within one cluster [10]. However, there are still two key problems that need to be clarified:

1) What is the relation between the CDS small-signal stability and the circulating currents?
2) What is the general approach to suppressing the CDS circulating currents?

The rest of this paper is organized as follows. Section II derives the closed-loop model of CDS. Section III transforms the CDS into two decoupled systems and proves that one of them reflects the circulating currents between GFMCs, while the other reflects the dynamics between the CDS and the infinite bus. Based on this analysis, we propose an approach to guide the suppression of circulating currents. Simulation results are given in Section IV. Section V concludes the paper.

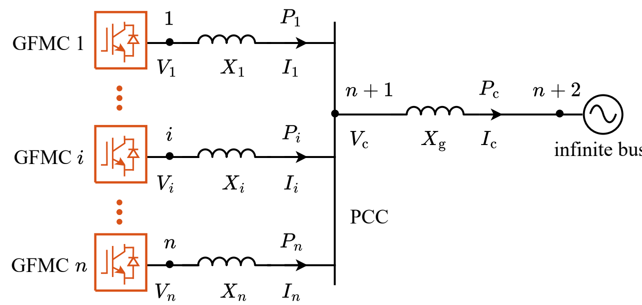

Fig. 1: Topology of CDS with parallel GFMC interconnection.

II. SMALL-SIGNAL STABILITY ANALYSIS OF CDS

A. Power System Model

As shown in Fig. 1, we consider a CDS that contains n GFMCs, parallel-configured at a point of common coupling (PCC). In what follows, the small-signal stability analysis is based on impedance/admittance modeling in the global synchronization coordinate system, i.e., the xy-axes. To model one GFMC module, without loss of generality, we employ the virtual synchronous generator control technology, which emulates the rotor motion equation and the voltage-source external characteristics. The detailed control diagram is de-

This work was supported by the Natural Science Foundation of China (No.U24B6008).*(Corresponding author: Linbin Huang.)*

Hangyu Chen, Kehao Zhuang, Liangxiao Luo, Huanhai Xin, and Linbin Huang are with the College of Electrical Engineering, Zhejiang University, Hangzhou 310027, China. (Emails: {hangyu.chen, zhuangkh, luolx, xinhh, hlinbin}@zju.edu.cn)

Verena Häberle is with the Automatic Control Laboratory, ETH Zurich, Zurich 8092, Switzerland. (Emails: verenhae@ethz.ch)

979-8-3315-8138-1

rived in reference [11]. Linearized at the operating point, the impedance model of the i-th GFMC can be expressed as

$$\Delta V_i = -Z_{\mathrm{a},i}(s)\Delta I_i, \tag{1}$$

where V_i, I_i and $Z_{\mathrm{a,i}}(s)$ are the i-th converter's xy-axes voltage vector, output current vector and impedance matrix respectively, Δ indicates the small-signal quantity, and s represents the Laplacian operator. The multi-device impedance model of the entire CDS can be established as

$$\Delta V = -Z_{\mathrm{A}}(s)\Delta I, \tag{2}$$

where $I := [I_1^{\mathrm{T}}, I_2^{\mathrm{T}}, \cdots, I_n^{\mathrm{T}}]^{\mathrm{T}} \in \mathbb{R}^{2n}$ is the GFMC current vector, $V := [V_1^{\mathrm{T}}, V_2^{\mathrm{T}}, \cdots, V_n^{\mathrm{T}}]^{\mathrm{T}} \in \mathbb{R}^{2n}$ is the voltage vector, $Z_{\mathrm{A}}(s) := \mathrm{diag}(Z_{\mathrm{a},1}(s), \cdots, Z_{\mathrm{a},n}(s))$ is the impedance matrix containing all GFMCs, and $\mathrm{diag}(\cdot)$ represents a block-diagonal transfer matrix.

For the modeling of the power network, i.e., the transmission lines between the GFMC units, in Fig. 1, the resistance-inductance ratio $\mu = R_i/X_i$ of the lines is assumed to be constant, the impedance from the PCC to the infinite bus is donated by X_{g}, the impedance from each node i to the PCC X_i is assumed to be equal to X_{a}. The infinite power grid (cf. node $n+2$ in Fig. 1) can be modeled as equivalent to the ground in small-signal stability analysis. So the susceptance matrix of the network is $B \in \mathbb{R}^{(n+1)\times(n+1)}$ can be divided as

$$B = \begin{bmatrix} \mathcal{I}_n/X_{\mathrm{a}} & -\mathcal{E}_n/X_{\mathrm{a}} \\ -\mathcal{E}_n^{\mathrm{T}}/X_{\mathrm{a}} & n/X_{\mathrm{a}} + 1/X_{\mathrm{g}} \end{bmatrix},$$

where $\mathcal{I}_n \in \mathbb{R}^{n\times n}$ is an identity matrix, $\mathcal{E}_n := [1, \cdots, 1]^{\mathrm{T}} \in \mathbb{R}^n$ is a all-one collomn vector. The interior node (node $n+1$) can be eliminated by Kron-Reduction [12], and the reduced susceptance matrix $\mathcal{B} \in \mathbb{R}^{n\times n}$ simplifies to

$$\begin{aligned} \mathcal{B} &= \frac{1}{X_{\mathrm{a}}}\mathcal{I}_n - \frac{\mathcal{E}_n}{X_{\mathrm{a}}}\left(\frac{n}{X_{\mathrm{a}}} + \frac{1}{X_{\mathrm{g}}}\right)^{-1}\frac{\mathcal{E}_n^{\mathrm{T}}}{X_{\mathrm{a}}} \\ &= \frac{1}{X_{\mathrm{a}}}\mathcal{I}_n - \frac{1}{X_{\mathrm{a}}}\frac{1}{n+\eta}\mathcal{J}_n, \end{aligned} \tag{3}$$

where $\eta := X_{\mathrm{a}}/X_{\mathrm{g}} \in \mathbb{R}^+$, $\mathcal{J}_n := \mathcal{E}_n\mathcal{E}_n^{\mathrm{T}} \in \mathbb{R}^{n\times n}$ is an all-ones square matrix. Therefore, the small-signal dynamics of the power network can be expressed as

$$\Delta I = Y_{\mathrm{N}}(s)\Delta V, \tag{4}$$

where $Y_{\mathrm{N}}(s) = \mathcal{B} \otimes F(s)$,

$$F(s) = \begin{bmatrix} s/\omega_0 + \mu & -1 \\ 1 & s/\omega_0 + \mu \end{bmatrix}^{-1}$$

is a 2×2 transfer matrix encoding the small-signal dynamics of an RL-line [13], and $\otimes$ denotes the Kronecker product.

B. Small-signal stability analysis

Based on (2) and (4), the CDS interconnection can be expressed as a closed-loop system $Z_{\mathrm{A}}(s)\#Y_{\mathrm{N}}(s)$ in Fig. 2. Since $Z_{\mathrm{A}}(s), Y_{\mathrm{N}}(s) \in \mathcal{RH}_\infty^{2n\times 2n}$ and there are no right-half pane pole-zero cancellations between $Z_{\mathrm{A}}(s)$ and $Y_{\mathrm{N}}(s)$. The closed-loop dynamics $Z_{\mathrm{A}}(s)\#Y_{\mathrm{N}}(s)$ is internally feedback stable if

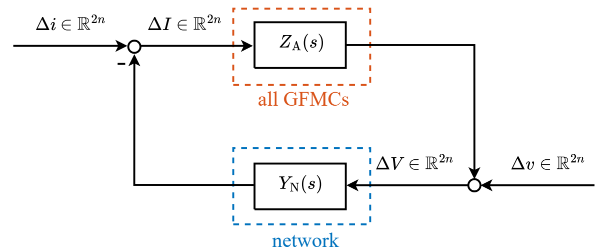

Fig. 2: The closed-loop feedback interconnection of the CDS dynamics.

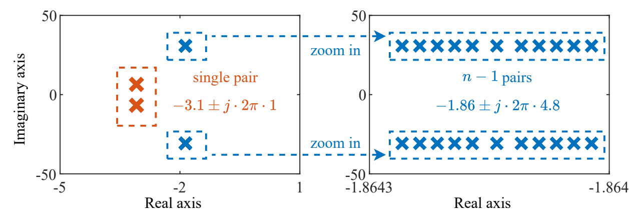

Fig. 3: The poles of $S(s)$ that dominate stability.

its sensitivity transfer function $S(s) := \mathcal{I}_{2n} + Z_{\mathrm{A}}(s)Y_{\mathrm{N}}(s)$ is stable [14]. Consider the CDS as shown in Fig. 1 whose corresponding parameters are listed in Table I, we plot the pole map of $S(s)$ (see Fig. 3), which contains two groups of poles. One group consists of a single pair of complex-conjugate poles (indicated in orange), and the other consists of $n-1$ complex-conjugate pole pairs (indicated in blue). The next subsection will show that the $n-1$ pairs of nearly overlapping poles actually reflect the circulating currents in CDS.

C. Circulating Current

According to the definition of circulating currents in the parallel connection of multiple GFMCs [15], the i-th circulating current of GFMC i is defined as the actual output current of GFMC i minus the converter's ideal output current I_0, i.e., $\tilde{I}_i = I_i - I_0$, where $I_0 = \sum_{i=1}^{n} I_i/n$. By defining the transformation matrix $T_{\mathrm{o}} := \mathcal{I}_n - \mathcal{J}_n/n$, the CDS's circulating currents can be expressed in matrix form

$$\tilde{I} = T_{\mathrm{o}} I, \tag{5}$$

where $\tilde{I} := [\tilde{I}_1^{\mathrm{T}}, \tilde{I}_2^{\mathrm{T}}, \cdots \tilde{I}_n^{\mathrm{T}}]^{\mathrm{T}}$is the vector of circulating currents. By definition, the sum of all converter circulation $\sum_{i=1}^{n} \tilde{I}_i = 0$, which means these circulating currents only flow within the parallel branches between all GFMCs and not into the remaining power grid. Here, $\mathrm{rank}(T_{\mathrm{o}}) = n-1$, which means T_{o} is essentially an irreversible mapping from the original current space to the circulating current space. For example, when $n = 2$, circulating current $\tilde{I}_1 = I_1/2 - I_2/2$ and $\tilde{I}_2 = I_2/2 - I_1/2$ are equal in magnitude and opposite in direction. Note that only one circulating current can't characterize the whole dynamics in the two-machine parallel system. Usually, we additionally consider the ideal output current $I_0 = I_1/2 + I_2/2$ to characterize the whole system dynamics.

Similarly, it is demonstrated that an n-machine parallel system requires $n-1$ circulating currents and an ideal output

979-8-3315-8138-1

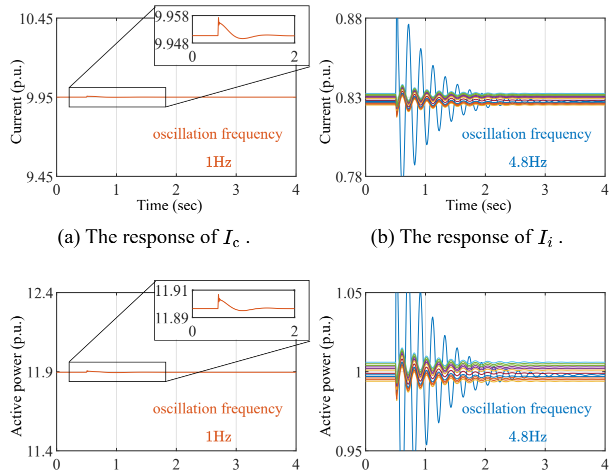

(a) The response of I_{c} .

(b) The response of I_i .

(c) The response of P_{c} .

(d) The response of P_i .

Fig. 4: The responses of CDS after a disturbance.

current to fully characterize its dynamics. We replace the last element of the vector $\tilde{I}$ with I_0 to get the extended circulating current vector $\tilde{I}_{\mathrm{e}} := \tilde{I} - \mathcal{A}_n \tilde{I}_n + \mathcal{A}_n I_0$. And we replace the elements of the last row of the T_{o} with $1/n$ to get the extended transformation matrix $T_{\mathrm{e}} := T_{\mathrm{o}} - \mathcal{A}_n \mathcal{A}_n^{\mathrm{T}} T_{\mathrm{o}} + \mathcal{A}_n \mathcal{E}_n^{\mathrm{T}}/n$, where $\mathcal{A}_n := [0, 0, \cdots, 0, 1]^{\mathrm{T}} \in \mathbb{R}^n$. With this, we rewrite (5) as

$$\tilde{I}_{\mathrm{e}} = T_{\mathrm{e}} I. \tag{6}$$

Thus, the sensitivity function for the extended circulating currents is $T_{\mathrm{e}} S(s) T_{\mathrm{e}}^{-1}$. Here, T_{e} is full rank so that $\det(T_{\mathrm{e}}) \neq 0$ and $\det(T_{\mathrm{e}} S(s) T_{\mathrm{e}}^{-1}) = \det(T_{\mathrm{e}})\det(S(s))\det(T_{\mathrm{e}}^{-1}) = \det(S(s))$. Therefore, the poles in Fig. 3 can reflect both the stability of the GFMC cluster output current and the stability of the circulating current between the GFMCs.

We can gain a more intuitive understanding of this conclusion through time-domain simulations. Consider a CDS whose topology is the same as in Fig. 1 with the closed-loop interconnection as in Fig. 3, and the corresponding parameters are listed in Table I. The current and active power responses of all converters (I_i, P_i) and the GFMC cluster (I_{c}, P_{c}) are monitored as shown in Fig. 4. After a power angle disturbance of the GFMC 1 at $t = 0.5$ s, the oscillation frequency of I_{c} and P_{c} is 1 Hz (related to the single pair of poles in Fig. 3), while the oscillation frequency of $I_{xy,i}$ and P_i is 4.8 Hz (related to the $n-1$ pairs of poles in Fig. 3). The 4.8Hz oscillation can't be monitored by I_{c} or P_{c}, which is another evidence that this mode is a circulating oscillation.

III. Circulating Currents Suppression in CDS

A. Decoupling of the of CDS Dynamics

We analyze the small-signal stability of CDS based on (2) and (4). The power angle difference of each GFMC is tiny,

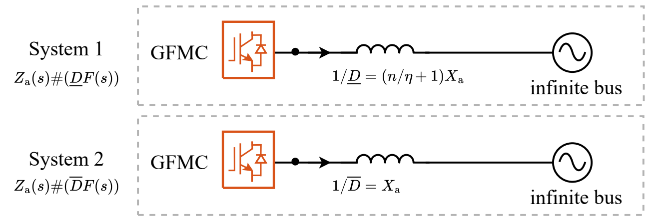

Fig. 5: Two decoupled interconnection systems.

and can be considered to be equal, i.e., $Z_{\mathrm{a},i}(s) = Z_{\mathrm{a}}(s)$. So the $\det(S(s)) = 0$ can be simplify as

$$\begin{aligned} &\det(\mathcal{I}_{2n} + Z_{\mathrm{A}}(s) Y_{\mathrm{N}}(s)) = 0 \\ \Longleftrightarrow\ &\det(\mathcal{I}_n \otimes Z_{\mathrm{a}}^{-1}(s) + \mathcal{B} \otimes F(s)) = 0 \\ \Longleftrightarrow\ &\det(\mathcal{I}_n \otimes Z_{\mathrm{a}}^{-1}(s) + \mathcal{D} \otimes F(s)) = 0 \\ \Longleftrightarrow\ &\textstyle\prod_{i=1}^{n} \det(Z_{\mathrm{a}}^{-1}(s) + D_i F(s)) = 0, \end{aligned} \tag{7}$$

where $\mathcal{D}$ is the diagonalized matrix derived from $\mathcal{B}$ by matrix eigenvalue decomposition, whose elements $\{D_i | i \in 1, 2, \cdots, n\}$ are the eigenvalues of $\mathcal{B}$. Considering the $\mathcal{B}$ matrix in (3), we can find that $\mathcal{B}$ is a symmetric Toeplitz matrix with diagonal elements e_{d} and non-diagonal elements e_{n}, where

$$e_{\mathrm{d}} = \frac{1}{X_{\mathrm{a}}} - \frac{1}{X_{\mathrm{a}}} \frac{1}{n+\eta} = \frac{n-1+\eta}{X_{\mathrm{a}}(n+\eta)},$$
$$e_{\mathrm{n}} = -\frac{1}{X_{\mathrm{a}}} \frac{1}{n+\eta}.$$

According the symmetric Toeplitz matrix eigenvalue theory [16], we can calculate the eigenvalues of the $\mathcal{B}$ matrix, one of which is $\underline{D} := e_{\mathrm{d}} + (n-1) e_{\mathrm{n}} = 1/(X_{\mathrm{a}}(n/\eta + 1))$, and $n-1$ of them are $\overline{D} := e_{\mathrm{d}} - e_{\mathrm{n}} = 1/X_{\mathrm{a}}$. Therefore, the steps to suppress circulating currents is as follows:

1) To assess the overall CDS's stability via (7), we divide matrix $\mathcal{B}$ eigenvalues, i.e., $\{D_i | i \in 1, 2, \cdots, n\}$, into two groups $\underline{D}$ and $\overline{D}$.
2) This allows us to decouple the CDS into two separate systems as shown in Fig. 5, where System 2 reflects the circulating currents.
3) By ensuring stability of System 2, we can suppress circulating currents.

Define a map $\mathcal{M} : \eta \to M$ that maps η to the decoupled interconnection system set M. Combine (7) and the value of $\underline{D}$ and $\overline{D}$, we have

$$\begin{aligned} M(\eta) =& \{Z_{\mathrm{a}}(s) \# \underline{D} F(s)\} \bigcup \{Z_{\mathrm{a}}(s) \# \overline{D} F(s)\} \\ =& \{Z_{\mathrm{a}}(s) \# \frac{F(s)}{(n/\eta + 1) X_{\mathrm{a}}}\} \bigcup \{Z_{\mathrm{a}}(s) \# \frac{F(s)}{X_{\mathrm{a}}}\}. \end{aligned} \tag{8}$$

When $\eta = X_{\mathrm{a}}/X_{\mathrm{g}} \to +\infty$, (8) converges to

$$M(+\infty) = \{Z_{\mathrm{a}}(s) \# \frac{F(s)}{X_{\mathrm{a}}}\}, \tag{9}$$

which can also be verified in Fig. 6. Mathematically, the ordinary set in (8) and the set in (9) are homotopic, and the map $\mathcal{M}$ is their homotopy [17]. This homotopy equivalence

979-8-3315-8138-1

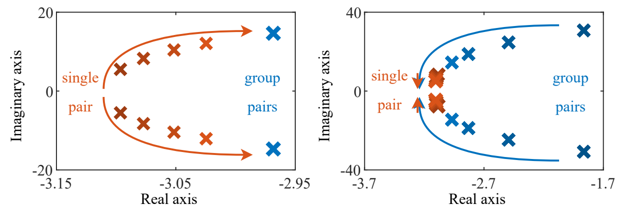

(a) Decrease X_{g} (increase η). (b) Increase of X_{a} (increase η).

Fig. 6: The pole map of $S(s)$. (a) $X_{\mathrm{a}} = 0.2$, $\eta \in (4.8, +\infty)$. (b) $X_{\mathrm{g}} = 0.042$, $\eta \in (1.2, +\infty)$.

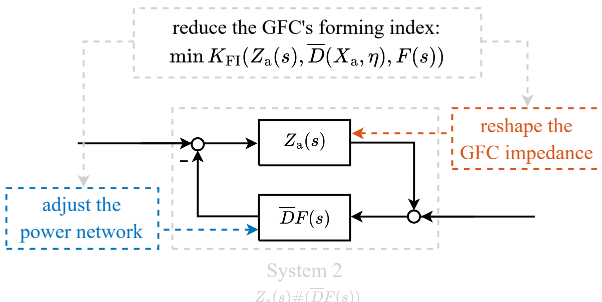

Fig. 7: Circulating currents suppression approach.

relation is attributed to the topological invariance of the CDS system power network during the continuous variation of η. It is consistent with physical intuition that the scenario in (9) corresponds to the scenario where all GFMCs are almost directly connected to the infinite bus, thereby verifying the correctness of CDS's dynamics decoupling.

B. Circulating Currents Suppression Approach of CDS

Thanks to the special property of Toeplitz matrices, the CDS can be decoupled into two systems, as shown in Fig. 5. The CDS is small-signal stable if and only if System 1 and System 2 are stable. Usually, the GFMC is prone to instability under a strong grid, but more stable under a weak network [18]. Therefore, if System 2 is stable, then System 1 is also stable, which means that the CDS small-signal stability is dominated by System 2, corresponding to circulating currents.

Theoretically, making the dominant pole of System 2 move as far to the left as possible can suppress the CDS circulating currents. However, from a practical point of view, it is more feasible to use some index to guide the suppression of circulating currents in CDS. Here, we choose the $\mathcal{H}_\infty$ norm of $Z_{\mathrm{a}}(s)\#\overline{D}F(s)$, the so-called forming index [19]

$$K_{\mathrm{FI}} := ||\mathcal{I}_2 + Z_{\mathrm{a}}(s)\overline{D} \otimes F(s)||_\infty \tag{10}$$

to suppress the circulating currents. Therefore, reducing K_{FI} as $\min K_{\mathrm{FI}}(Z_{\mathrm{a}}(s), \overline{D}(X_{\mathrm{a}}, \eta), F(s))$ is an approach to suppress the circulating currents in CDS. And there are two ways to suppress the circulating currents (see Fig. 7). One way is to redesign the GFMC control to align with the line dynamics $\overline{D}F(s)$. The other way is to adjust the power network line parameters to align with the GFMC impedance $Z_{\mathrm{a}}(s)$.

Notably, grid-following converters are usually stable under a strong grid but unstable under a weak grid. Therefore, the

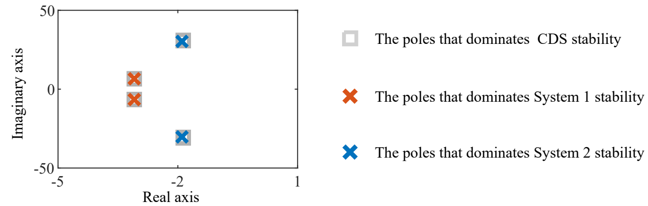

Fig. 8: The poles of CDS, System 1 and System 2 that dominate stability.

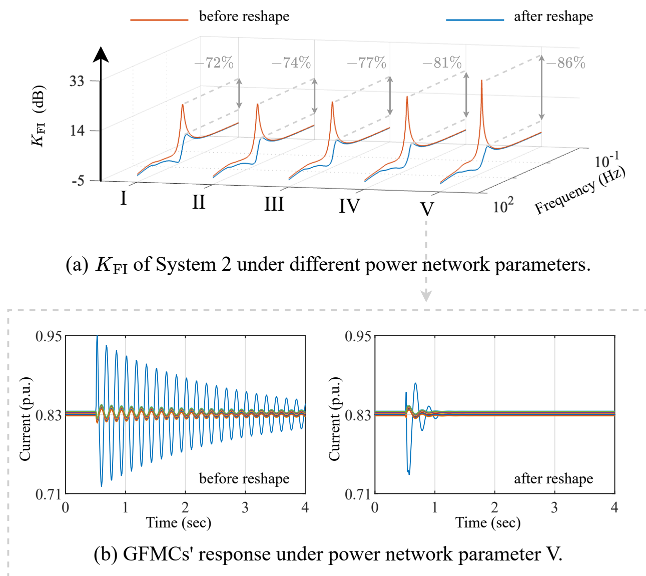

(a) K_{FI} of System 2 under different power network parameters.

(b) GFMCs' response under power network parameter V.

Fig. 9: Suppressing circulating currents by reshaping the GFMC impedance.

stability of a grid-following converter cluster is dominated by System 1. It is consistent with the fact that grid-following converters typically do not experience circulation problems caused by clusters, but rather small-signal instability issues associated with long grid-connected lines.

IV. Simulation Verification

In this section, we will validate the proposed small-signal stability analysis and the suppression approach of circulating currents. The corresponding parameters are listed in Table I.

To validate the dynamics decoupling of CDS, we plot the dominant pole map of CDS, System 1, and System 2, as shown in Fig. 8. The $\times$ markers and $\square$ markers are overlapped, which means the two decoupled interconnection systems established in Fig. 5 perfectly characterize the dynamics of the CDS in Fig. 1.

To validate the proposed approach, we verify it from two aspects. On the one hand, we redesign the GFMC impedance to align with the line $\overline{D}F(s)$. As shown in Fig. 9 (a), by reshaping the GFMC impedance, K_{FI} can be effectively reduced under five different power network parameters. Furthermore, we simulate the CDS under parameter V in Fig. 9 (b). We found that the circulating current of the CDS was significantly

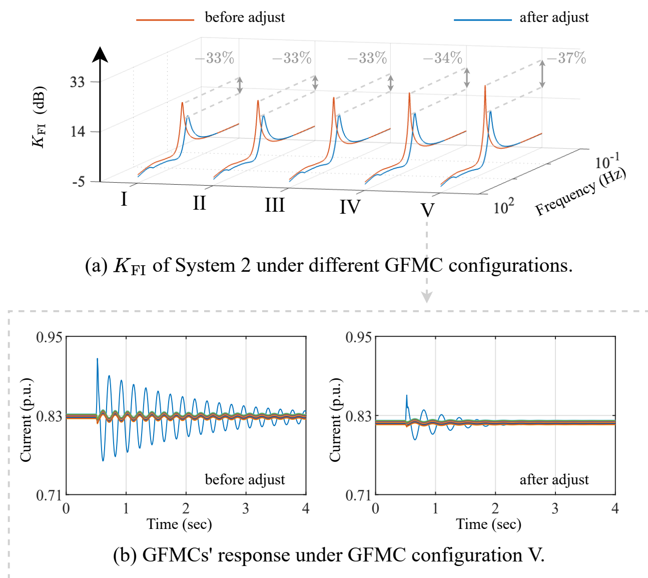

Fig. 10: Suppressing circulating currents by adjusting the power network.

suppressed after GFMC impedance reshaping. On the other hand, we adjust the power network to align with the GFMC. As shown in Fig. 10 (a), by adjusting the power network parameter, K_{FI} can be effectively reduced under five different GFMC configurations. Furthermore, we simulate the CDS under configuration V in Fig. 10 (b). We found that the circulating current of the CDS was significantly suppressed after adjusting the power network parameters.

V. Conclusions

This paper has addressed the challenges of small-signal stability and circulating currents in a CDS fully configured with GFMCs. By establishing the closed-loop system dynamics and employing a matrix eigenvalue decomposition, the CDS can be decoupled. A key finding was the theoretical proof that one of them directly governs the behavior of circulating currents. A corresponding suppression approach was proposed. Simulation results have conclusively validated the effectiveness of the proposed analysis and suppression approach. This work paves the way for ensuring high penetration of GFMC integration and modular construction in future power systems.

TABLE I: Configuration of CDS

Power network parameters (p.u.)	
GFMC number	$n = 12$
Resistance-inductance ratio	$\mu = 0.05$
Impedance from node $n+1$ to $n+2$	$X_{\mathrm{g}} = 0.06$
Impedance from node $i \in \{1, \cdots, n\}$ to $n+1$	$X_{\mathrm{a}} = 0.05$

GFMC configurations (p.u.)	
Filter inductor	0.05
Filter capacitor	0.05
Active power reference	1.0
Voltage reference	1.1
Virtual inertia coefficient	8
Virtual damping coefficient	50
Other control configurations refer to reference [11]	

Power network parameters I-V in Fig. 9 (p.u.)	
Grid-side impedance	0.055 : 0.005 : 0.035

GFMC configurations I-V in Fig. 10 (p.u.)	
Virtual damping coefficient	50 : 5 : 30

References

[1] F. Milano, F. Dorfler, G. Hug, D. J. Hill, and G. Verbia, "Foundations and challenges of low-inertia systems (invited paper)," in *2018 Power Systems Computation Conference (PSCC)*, 2018, pp. 1–25.

[2] H. Xin *et al.*, "How many grid-forming converters do we need? a perspective from small signal stability and power grid strength," *IEEE Trans. Power Syst.*, pp. 1–13, 2024.

[3] G. Mu, F. Wu, X. Zhang, Z. Fu, and B. Xiao, "Analytic mechanism for the cumulative effect of wind power fluctuations from single wind farm to wind farm cluster," *CSEE J. Power Energy Syst.*, vol. 8, no. 5, pp. 1290–1301, 2022.

[4] J. Yang and C. Tse, *Complex Behavior of Grid-Connected Power Electronics Systems*. Springer Nature Switzerland, 2024.

[5] V. Häberle, A. Tayyebi, X. He, E. Prieto-Araujo, and F. Dörfler, "Grid-forming and spatially distributed control design of dynamic virtual power plants," *IEEE Trans. Smart Grid*, vol. 15, no. 2, pp. 1761–1777, 2024.

[6] V. Häberle, M. W. Fisher, E. Prieto-Araujo, and F. Dörfler, "Control design of dynamic virtual power plants: An adaptive divide-and-conquer approach," *IEEE Trans. Power Syst.*, vol. 37, no. 5, pp. 4040–4053, 2022.

[7] S. Liao, M. Huang, X. Zha, and J. M. Guerrero, "Emulation of multi-inverter integrated weak grid via interaction-preserved aggregation," *IEEE J. Emerg. Sel. Top. Power Electron.*, vol. 9, no. 4, pp. 4153–4164, 2021.

[8] J. Zhang, Y. Liu, Y. Wei, X. Zhang, and Z. Wu, "Virtual composite impedance circulating current suppression strategy with adaptive adjustment capability," *IET Gener. Transm. Distrib.*, vol. 17, no. 15, pp. 3376–3388, 2023.

[9] R. Babazadeh-Dizaji, M. Hamzeh, and K. Sheshyekani, "A consensus-based cooperative control for dc microgrids interlinked via multiple converters," *IEEE Syst. J.*, vol. 15, no. 4, pp. 4918–4926, 2021.

[10] S. Liao, Y. Chen, W. Wu, L. Wang, and Q. Xu, "Closed-loop interconnected model of multi-inverter-paralleled system and its application to impact assessment of interactions on damping characteristics," *IEEE Trans. Smart Grid*, vol. 14, no. 1, pp. 41–53, 2023.

[11] L. Huang, H. Xin, and Z. Wang, "Damping low-frequency oscillations through vsc-hvdc stations operated as virtual synchronous machines," *IEEE Trans. Power Electron.*, vol. 34, no. 6, pp. 5803–5818, 2019.

[12] F. Dörfler and F. Bullo, "Kron reduction of graphs with applications to electrical networks." *IEEE Trans. Circuits Syst.*, vol. 60, no. 1, pp. 150–163, 2013.

[13] V. Häberle, X. He, L. Huang, F. Dörfler, and S. Low, "Decentralized parametric stability certificates for grid-forming converter control," 2025. [Online]. Available: https://arxiv.org/abs/2503.05403

[14] S. Skogestad and I. Postlethwaite, *Multivariable feedback control: analysis and design*. Wiley New York, 2007, vol. 2.

[15] C.-T. Pan and Y.-H. Liao, "Modeling and coordinate control of circulating currents in parallel three-phase boost rectifiers," *IEEE Trans. Ind. Electron.*, vol. 54, no. 2, pp. 825–838, 2007.

[16] R. Horn and C. Johnson, *Matrix Analysis*, ser. Matrix Analysis. Cambridge University Press, 2013.

[17] W. Rudin, *Functional Analysis*, ser. International series in pure and applied mathematics. McGraw-Hill, 1991.

[18] H. Chen *et al.*, "Damping enhancement control of virtual synchronous generator based on dynamic virtual impedance," *High Volt. Eng.*, vol. 51, no. 02, pp. 570–580, 2025.

[19] K. Zhuang *et al.*, "Quantifying grid-forming behavior: Bridging device-level dynamics and system-level stability," 2025. [Online]. Available: https://arxiv.org/abs/2503.24152